Renewable surface fluorescence sandwich immunoassay biosensor for rapid sensitive botulinum toxin detection in an automated fluidic format

Jay W. Grate,*[a] Marvin G. Warner,[a] Richard M. Ozanich, Jr.,[a] Keith D. Miller,[a] Heather A. Colburn,[a] Brian Dockendorff,[a] Kathryn C. Antolick,[a] Norman C. Anheier Jr.,[a] Michael A. Lind,[a] Jianlong Lou,[b] James D. Marks[b] and Cynthia J. Bruckner-Lea[a]

Received 14th January 2009, Accepted 17th February 2009
First published as an Advance Article on the web 5th March 2009
DOI: 10.1039/b900794f

A renewable surface biosensor for rapid detection of botulinum neurotoxin serotype A is described based on fluidic automation of a fluorescence sandwich immunoassay, using a recombinant protein fragment of the toxin heavy chain (~50 kDa) as a structurally valid simulant. Monoclonal antibodies AR4 and RAZ1 bind to separate non-overlapping epitopes of the full botulinum holotoxin (~150 kDa). Both of the targeted epitopes are located on the recombinant fragment. The AR4 antibody was covalently bound to Sepharose beads and used as the capture antibody. A rotating rod flow cell was used to capture these beads delivered as a suspension by a sequential injection flow system, creating a 3.6 μL column. After perfusing the bead column with sample and washing away the matrix, the column was perfused with Alexa 647 dye-labeled RAZ1 antibody as the reporter. Optical fibers coupled to the rotating rod flow cell at a 90° angle to one another delivered excitation light from a HeNe laser (633 nm) using one fiber and collected fluorescent emission light for detection with the other. After each measurement, the used Sepharose beads are released and replaced with fresh beads. In a rapid screening approach to sample analysis, the toxin simulant was detected to concentrations of 10 pM in less than 20 minutes using this system.

Introduction

Botulinum neurotoxin (BoNT) is among the most poisonous substances known to man.[1–7] Human exposure can occur through inadvertent exposure to contaminated foods or through intentional acts of terrorism or warfare. The gold standard for botulinum toxin detection is the mouse bioassay, a functional assay at the whole animal level, which requires days to detect positives.[7–10] It has a detection limit of 10–20 pg/mL (15 pg/mL corresponds to 0.10 pM for the 150 kDa toxin protein). Enzyme-linked immunoassays (ELISAs), where enzymatic catalysis provides amplification, are capable of sensitive detection but typically require 3–8 hours.[11–13] The ELISAs are structure-based assays requiring affinity reagents such as antibodies with specificities toward the botulinum toxin. Both the mouse bioassay and ELISA methods are capable of detecting botulinum toxin to concentrations of 1 pM or less in buffer solutions or sample matrixes that do not interfere. A sensitive enzyme-amplified assay has been implemented in a microarray format, requiring 2–5 hours.[14] Immuno-PCR approaches, where nucleic acids are amplified after immunochemical recognition, represent another sensitive, albeit time-consuming, detection method.[15] Assays have also been developed that detect the proteolytic activity of the toxin.[16–19] These are functional assays at the molecular level and require that the holotoxin be intact and that the catalytic site responsible for the toxicity of the botulinum toxin be present. Assays for botulinum toxin were reviewed in two articles in 2005,[7,10] and both indicated a continuing need for assays to replace the mouse bioassay and enable rapid screening of large numbers of samples. A number of promising new assay formats have appeared recently[20–28] that provide assays that are sensitive or fast. However, assays that are both fast and sensitive remain desirable in many applications.

Test strips represent an immunoassay format commonly used for rapid analysis. However, most such approaches for BoNT are not very sensitive. Gessler *et al.* evaluated four commercial lateral flow assays, each taking 15 minutes.[29] The best detection limit for purified toxin serotype A (see below) was 50 ng/mL, while detection limits of 10 ng/mL for toxin complex were found for two of the test strips. Sharma *et al.* also evaluated lateral flow assays obtaining detection limits of 10 ng/mL.[30] Han *et al.* reported a detection limit of 100 ng/mL for a 15 minute lateral flow assay, and demonstrated a 2 ng/mL detection limit using a cross-flow method they developed for a rapid ELISA taking about 20 minutes.[21] By contrast, however, Ahn-Yoon *et al.* have described a lateral flow assay using liposome labels containing 10^5 dye molecules for amplification; a detection limit of just 15 pg/mL in 20 minutes was reported.[22]

A rapid biosensor using a fiber optic evanescent wave detection approach achieved a 30 pM detection limit for botulinum toxin A in an immunoassay that took less than 20 minutes.[31,32] This work, reported in 1992 and 1993, is arguably the first rapid and sensitive assay for botulinum toxin. Fluidic array biosensors have been reported more recently, achieving detection limits of 20 ng/mL (100 pM) in 20 minutes.[33,34] Recently, Attree *et al.* described a lateral flow assay, and compared it with a small disposable immunochromatography column set up to carry out

[a]*Pacific Northwest National Laboratory, P. O. Box 999, Richland, WA 99352, USA*
[b]*University of California, Department of Anesthesia, Rm 3C-38, NH, 1001 Potrero, San Franscisco, CA 94110, USA*

an enzyme-amplified immunoassay with precipitating TMB for color development.[20] These authors reported a 20–40 pM detection limit for the lateral flow assay in 40 minutes, and achieved an impressive 0.45 pM detection limit using their new immunochromatography approach, again in 40 minutes. Sample, reagent and wash solutions were added manually to the column and allowed to flow by gravity.

In this paper we describe a rapid fluorescence sandwich immunoassay for the detection of botulinum toxin in an automated microcolumn sensor configuration. A fluorescence sandwich immunoassay avoids the time-consuming delays associated with amplification procedures. The assay is set up as a solid phase immunoassay where the capture antibodies are immobilized on Sepharose beads, as shown in Fig. 1. These beads are fluidically packed in a microcolumn sensor using a renewable surface technique derived from the field of flow injection and sequential injection (SI) analysis.[35–41] It has also been called 'bead injection', and a variety of flow cells have been developed.[35,37,39,42–47] This method is illustrated in Fig. 2, using a 'rotating rod' flow cell[43,44] fitted with optical fibers for on-column detection. The fluorescent sandwich complex is assembled and purified in this column

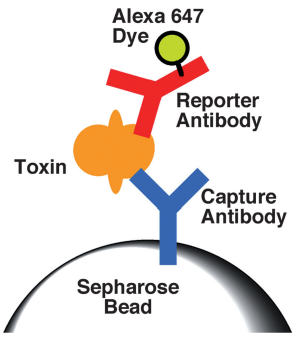

Fig. 1 Schematic diagram for the sandwich immunoassay complex for botulinum toxin detection, illustrated with capture and reporter antibodies binding to the same subunit of a toxin molecule. In our assay, we used a fragment of the toxin that contains the same epitopes as the full toxin for binding both the capture and reporter antibodies.

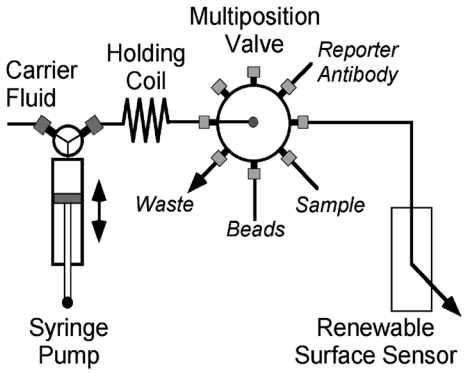

Fig. 3 Schematic diagram of the sequential injection system with the rotating rod renewable surface sensor flow cell as the separator/reactor/detector. The actual multiposition valve was a 10-port valve with additional wash solutions and a port devoted to aspirating an air segment.

sensor by perfusing the beads with sample, wash, dye-labeled reporter antibody, and final wash solutions, using an SI system shown in Fig. 3 for programmed fluid delivery. The on-column fluorescence detection system monitors this process and detects the assembled and washed sandwich complex.

The renewable surface method enables the capture of Sepharose beads in the flow cell, prior to each assay, and the release of the used beads after the assay. In this way, the surface for biomolecular recognition is renewed for each sample or measurement, and the flow cell can be cleaned in between measurements without concern for the damaging effects that the cleaning solutions could cause to permanently placed biomolecular interfaces. Renewable surface methods have been used for immunoassays[14,38,44,48–53] and for separating biomolecules from complex sample matrixes.[45,54–57]

Botulinum toxin is a 150 kDa protein that occurs as seven serotypes designated with capital letters. Serotypes A, B, E, and F are toxic to humans. Our assay development has focused on the detection of botulinum toxin serotype A, abbreviated BoNT/A, which has a molecular weight of 150 kDa. The toxin can also be isolated as a toxin complex with various neurotoxin-

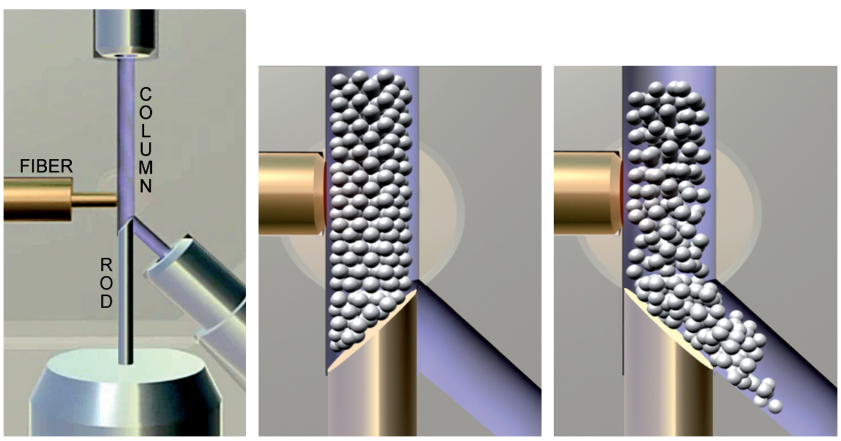

Fig. 2 (Left) The rotating rod flow cell: the cell is constructed of chlorotrifluoroethylene (CTFE) with a ~1.04 mm diameter column flow channel. (Center) A beveled nickel rod having a diameter of approximately 1 mm permits trapping of beads while allowing sample, reagents and wash solutions to be perfused over the bead column. Two fiber optics (in the same horizontal plane, and at 90° relative to each other) are integrated into the flow cell to allow laser excitation and fluorescence detection. (Right) After the assay is complete, the rod is rotated 180°, the beads are flushed to waste, and the flow cell is washed and rinsed.

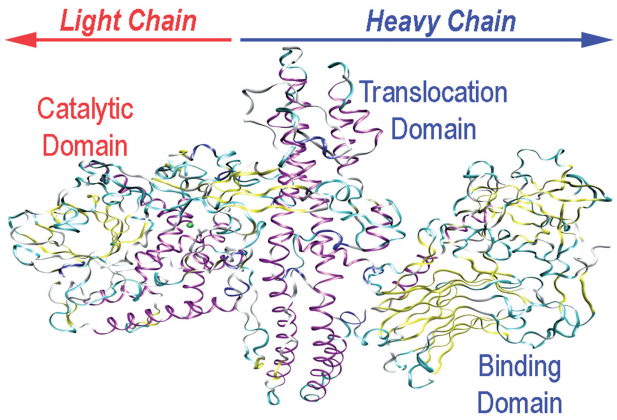

Fig. 4 Botulinum toxin image showing the three domains in two chains. The binding domain fragment of the heavy chain, produced by expression vector synthesis and expression in *Escherichia coli*, was used as a non-toxic simulant. The structure was rendered using POV-Ray rendering software from PDB ID: 3bta.[4]

associated proteins (NAPs) with a total molecular weight up to 900 kDa. The 150 kDa toxin protein has a heavy chain and a light chain that contain a total of three functional subunits, each about 50 kDa in size, as shown in Fig. 4. The heavy chain contains one subunit that is involved in recognition and binding to nerve cell surfaces, and another subunit that facilitates translocation of the toxin into the cell by receptor-mediated endocytosis. The light chain contains a single subunit of the toxin, a Zn^{2+}-containing protease. The action of this protease in the cell interferes with neurotransmitter release in neuromuscular junctions, leading to muscular paralysis.

The antibodies in our assay recognize epitopes located in the binding domain of the heavy chain.[58–64] We used a recombinant fragment of the heavy chain,[65,66] denoted here as BoNT/A-H_C-fragment, corresponding to the binding domain as a structurally valid simulant for the full BoNT/A for testing our assay. The antibodies have been demonstrated to bind to the BoNT/A holotoxin with affinities that are similar to or better than their interaction with the recombinant fragment.[62,64] The antibodies were developed using a phage display approach for single chain antibodies. Selection of antibodies with high affinity for the binding domain was followed by the use of molecular evolution techniques and yeast display methods to refine the affinity and selectivity of selected antibodies, leading to families of antibodies that bind to particular epitopes. These were constructed as IgG antibodies for use as reagents in our assays.

We have very briefly described the renewable surface assay for botulinum toxin previously.[14] We now describe the assay in detail after further development, with detection limits substantially below those reported before. In a rapid screening approach to be described, we have detected the toxin simulant to concentrations of 10 pM or less in 20 minutes.

Experimental

Commercial materials

NHS-activated Sepharose 4B Fast Flow beads were purchased from GE Amersham BioSciences (Uppsala, Sweden). Phosphate buffered saline (PBS) was obtained from Sigma-Aldrich (St Louis, MO). Fetal Bovine Serum (FBS) was obtained from Invitrogen Corporation (Grand Island, NY). Quick start Bradford dye reagent, 1X was purchased from Bio Rad Laboratories, Inc. (Hercules, CA). Bovine serum albumin (BSA), Fraction V was acquired from Fisher Scientific (Fair Lawn, NJ). Nunc-immuno polystyrene Maxisorp U96 microwell plates were obtained from Fisher Scientific (Pittsburg, PA). SuperBlock T20 (PBS) Blocking Buffer was purchased from Pierce Biotechnology (Rockford,CA); this buffer is a pH 7.4 PBS buffer containing 0.05% Tween-20 and a proprietary protein formulation. We used this buffer as the carrier fluid in our system, for washing steps, and to dilute reagents.

Capture and reporter antibodies

Antibodies to BoNT/A were obtained from Professor Jim D. Marks (University of California, San Francisco) who used a yeast display method for molecular evolution and selection of the antibodies.[58–63] Briefly, plasmids (genetic information) coding for a single chain variable fragment (scFv) are transformed into yeast. A yeast 'library' is produced that expresses scFv on their surface with a high degree of diversity. Antigen selections are used to 'pull out' the best binders. This molecular evolution or affinity maturation leads to better binders having higher affinities (lower K_D). Once a selected scFv has been affinity matured, it is converted to a full IgG. Two families of antibodies were produced which bind different epitopes on the binding domain. The C25 family includes AR1, AR2, and AR4 antibodies, of which AR4 was used as the capture antibody for this work. The 3D12 family included 3D12 and RAZ1 antibodies, of which RAZ1 was used as the reporter antibody.

Botulinum toxin simulant

The binding domain of the heavy chain of BoNT (BoNT/A-H_C-fragment)[65,66] was generated in-house by expression vector synthesis and expression in *E. coli*. Briefly, vector synthesis was performed by ligating *Clostridium botulinum* BoNT/A gene fragment into the NdeI/XhoI sites of pET28 downstream of the T7 promoter. The expressed protein has an N-terminal 6X-His tag that can be removed by thrombin cleavage to produce native protein. The *E. coli* expression method consisted of transforming the expression plasmid into BL21 (DE3) cells and inducing expression at 37 °C for 16 hours. The BoNT/A-H_C-fragment in the soluble fraction was immobilized onto Ni-NTA resins, washed, and eluted with imidazole. Ni eluate was de-salted and incubated with AEC resin. The flow-through was collected and BoNT/A-H_C-fragment was immobilized on CEC resin. Then, CEC resin was washed and BoNT/A-H_C-fragment was eluted with NaCl resulting in yields of approximately 100 mg/L. The activity of BoNT/A-H_C-fragment was verified by ELISA, Biacore, and BoNT/A-specific scFv antibody-coupled microbead assay with flow cytometry detection.

Capture antibody immobilization

AR4 capture antibodies were covalently linked to the surface of the NHS-activated beads as follows. A 300 μL suspension of NHS-activated Sepharose Fast Flow beads (provided in

isopropanol) were added to a 2 mL micro-centrifuge tube. The beads were centrifuged for 1.5 minutes at 13 000 rpm and the top isopropanol layer was removed. Per the manufacturer's instructions, the beads were washed three times with 300 μL of 1 mM HCl followed by three washes with 300 μL of PBS (Phosphate Buffered Saline: 0.01 M PBS, pH 7.4, 0.138 M NaCl, 0.0027 M KCl) by using centrifugation for 1.5 minutes at 13 000 rpm. After 200 μL of AR4 IgG antibody (0.8 to 1 mg/mL) and 100 μL of buffer were added to the tube, it was vortexed gently for 5 seconds and placed in the centrifuge for 1.5 min at 13 000 rpm. A 15 μL aliquot of supernatant was removed and stored in a separate labeled tube at 4 °C for a Bradford analysis. The beads in the remaining solution were then placed in an invert mixer for 12–24 hours at 4 °C. After the reaction was complete, the supernatant was removed by centrifugation for 1.5 minutes at 13 000 rpm and kept in a separate labeled tube for Bradford analysis. A 300 μL volume of Tris Buffered Saline (0.05 M Tris, pH 8.0, 0.138 M NaCl, 0.0027 M KCl) was then reacted with the beads in an invert mixer for 1 hour at 4 °C to block any remaining binding sites. The beads were then washed three times with buffer by centrifugation at 13 000 rpm for 1.5 minutes. 1 mL of buffer was added to the bead vial to make up the stock bead solution. The coupling efficiency was determined by performing a Bradford assay and analyzed at 595nm in a TECAN Safire plate reader. The Bradford assay was used to confirm removal of protein from solution due to coupling to the beads. Typical coupling efficiencies were greater than 90%. Nominally, 0.2 mg of antibody protein are contained in the 1 mL suspension.

Bradford assay

Protein standards were prepared in 1× PBS (0.08 M Na_2HPO_4, 0.02 M NaH_2PO_4, 0.138 M NaCl, 0.0027 M KCl adjusted to pH 7.4,) using bovine serum albumin (BSA) with concentrations of 1, 0.5, 0.25, 0.125, 0.0625 mg/mL. The first three rows of the 96 well plate were filled with 300 μL of Quick Start Bradford Dye Reagent, 1X. The reagent was kept in the dark until reaching room temperature. 5 μL of 1 mg/mL BSA standard was added to wells A1–C1 and mixed gently by pipette mixing. The other four concentrations of BSA were added to columns 2 thru 5 respectively. Each concentration was run in triplicate. In column 6, 5 μL of the first decant taken during the bead coupling was added to each well and pipette mixed. In column 7, 5 μL of the second decant taken during the bead coupling was added to each well and pipette mixed. In column 8, buffer was added to each well and pipette mixed. The plate was then placed in the TECAN plate reader. The absorbance was measured at 595 nm. The coupling efficiency was found by subtracting the initial protein concentration of the antibody added during the bead coupling minus the protein concentration of the solution after the coupling divided by the initial protein concentration.

Reporter antibody labeling

AlexaFluor® 647 fluorescent dye was covalently attached to RAZ1 antibodies by Invitrogen Molecular Probes (Eugene, OR). Mixing the amine-reactive succinimidyl ester form of the dye with antibody results in covalent attachment of the dye to the lysine and end-terminal amine groups on the antibody. The resulting dye-labeled antibody contained approximately 6.0 moles of dye per mole of antibody at a concentration of 0.90 mg/mL (0.1 M $NaHPO_4$, 0.1 M NaCl, 2 mM azide adjusted to pH 7.5). The stock solution was stored in the dark at 2–6 °C and working dilutions were made daily.

Renewable surface microcolumn sensor flow cell

The flow cell (Fig. 2) was machined in-house from chlorotrifluoroethylene (CTFE), obtained from McMaster-Carr (Atlanta, GA). 1 mm diameter nickel rod was purchased from Goodfellow Corporation (Oakdale, PA) and a 45° bevel was cut and polished on one end. Inlet and exit tubing (1/16″ OD, 1/32″ ID) was obtained from Upchurch Scientific (Oak Harbor, WA). Tubing fittings (062 MINSTAC) from The Lee Company (Westbrook, CT) were used for inlet and outlet ports on the flow cell. The flow channel column was drilled using a No. 60 (1.02 mm diameter) or No. 59 (1.04 mm diameter) drill bit such that it was approximately 20–40 μm larger than the nickel rod diameter. The rotating rod was computer-controlled using a National Instruments (Austin, TX) SCB-68 break-out board connected to a National Instruments DAQ-PAD 6020E communication package. The Arsape stepper motor (La Chaux-de-Fonds, Switzerland) was powered by a 12–24 V power supply (500 mA running, idle current is 15 mA) and was actuated by sending a 0 or 5 V signal from the SCB-68 to the Arsape driver board (AD VM M3) which controls the rod stepper motor.

Fluidic system

The fluidic system consisted of a sequential injection system as shown in Fig. 3. A 1 mL model XP3000 syringe pump (Cavro Scientific Instruments Inc., Sunnyvale, CA) with a 3-port valve was used as the fluid drive. The center (common) port of a 10-port Cheminert® stream selection valve (Valco Instruments Co. Inc. Houston, TX) was connected to the outlet port of the syringe pump valve with a 1 mL holding coil between them. All tubing was FEP (fluorinated ethylene propylene) 1/16 inch outside diameter × 0.030 inch inside diameter. In-house software to control the pump, valve, rotating rod, and data collection was written in LabWindows CVI (National Instruments, Austin, TX). SuperBlock T20 (PBS) Blocking Buffer was used as the carrier liquid (and for washing steps). The pump, holding coil, and selection valve were used to aspirate and dispense solutions containing the bead suspension, sample, or reporter antibody reagents. Each such solution was individually aspirated and dispensed to the column followed by a volume of wash solution.

Optical detection system

A 5.0 mW Helium-Neon laser (633nm emission) was used for fluorescence excitation (Thorlabs, Newton, NJ). Ocean Optics (Dunedin, FL) custom-machined low-OH (very low hydroxyl content) fiber optics (1 meter long, 600 μm core, polyimide buffer, 0.22 numerical aperture) were used to deliver light from the HeNe excitation laser to the flow cell and to collect the laser-induced fluorescence from the sample in the flow cell and direct it through a filter train to a Hamamatsu (Bridgewater, NJ) photomultiplier tube (PMT model H6779-20).

The custom-machined ends of the fiber optics were threaded to provide secure attachment to the flow cell. The end of the fiber protruded 2.5 mm and included an aluminium buffer cladding (fiber and cladding had a 810 μm outside diameter). This end of the fiber was press fit into the flow cell to provide a liquid tight seal. Light from the HeNe laser was directed through a Semrock (Rochester, NY) 633 nm MaxLine™ laser-line filter (part # LD01-640/8-12.5) prior to being delivered to the flow cell. Light from the collection fiber was directed through a filter train with the following components in the order listed: Collimation lens ('CL'; Thorlabs, Newton, NJ), 5 mm aperture ('AP'), 647 nm RazorEdge™ long-wave-pass filter ('RE'; Semrock part # LP02-633RU-25), 5 mm aperture ('AP'), 675 nm bandpass filter ('BP'; Chroma part # HQ675/50, Rockingham, VT), focusing lens ('FL'; Thorlabs, Newton, NJ), PMT.

A custom circuit board was designed for the PMT. The PMT signal was first amplified by a transimpedance op-amp stage with a gain of up to 10^7 and a time constant of 1 sec. This stage was followed by a standard non-inverting stage with a variable gain between 1 and 100. This gain was user adjustable by a potentiometer. This was useful for trimming the peak output voltage for maximizing the analog-to-digital converter resolution, although large gain settings on the secondary stage will also increase the noise. A gain of 67 was used on our experiments.

Assay procedure

The Sepharose beads with the capture antibody were diluted 1 : 10 from the stock using buffer (PBS 7.4). The reporter antibody was diluted from the stock solution described above (anti-RAZ1, human IgG2 AlexaFluor 647 0.9 mg/mL) by a factor 1 : 2000 (unless specified otherwise), *i.e.* to 0.45 μg/mL, using SuperBlock T20 (PBS) Blocking Buffer. Dilutions of the 2.2 mg/mL botulinum toxin fragment were made up in SuperBlock T20 (PBS) Blocking Buffer. All reagents were kept on ice in the dark. A 120 μL volume of diluted bead suspension was aspirated into the holding coil at 10 μL/sec and delivered to the CTFE flow cell at 5 μL/sec with the rotating rod in the trap position, resulting in a 3.6 μL packed bead column. 100μL of the BoNT/A-H_C-fragment simulant sample was dispensed over the column in 1 μL increments at 1μL/sec, with pauses between each such advance, followed by a 75 μL buffer wash (SuperBlock T20 (PBS) Blocking Buffer). After 100 μL of the dye-labeled reporter antibody were dispensed over the bead column, the unbound dye was washed out of the column by two different washes (25 μL at 1 μL/sec and 1900 μL at 5 μL/sec) using carrier solution (SuperBlock T20 (PBS) Blocking Buffer). The 1900 μL fast wash required filling the 1 mL syringe prior to the wash and again in the middle of the wash. The solutions delivered to the flow cell to carry out the assay are summarized in Table 1.

Table 1 Solutions delivered to the renewable surface sensor for a rapid screening assay

Approximate start time[a] (min)	Solution	Volume (μL)	Flow rate (μL/sec)
0	Wash with blocking solution	500	5
2	Sample (standard or blank)	100	1[a]
6	Sample wash	75	3
6.5	Reporter antibody	100	1[a]
10.5	Wash 1	25	1
11.5	Wash 2	1900	5

[a] The solution delivery steps above begin after the column has already been fluidically packed with antibody-coupled Sepharose beads. Flow was stopped and the 1 mL syringe was refilled prior to the beginning of the fast wash and again at the middle of the fast wash at approximately 15.5 min (total 1.9 mL). Programmed delays and brief stops in the procedure are not listed in the table. During sample perfusion and reporter antibody perfusion, the fluid was advanced 1 μL at a time at 1 μL/sec, with delays between each such advance to provide increased contact time. The total contact time with the microbead column for 100 μL sample and 100 μL reporter antibody was approximately 4 minutes each.

Results and discussion

Measurement approach

There are three key aspects to our measurement approach: (1) the immunoassay reagents; (2) the fluidic manipulation of solid phases, reagent solutions, and wash solutions to carry out a multistep immunoassay procedure automatically; and (3) an on-column detection system to record the fluorescent signals. The monoclonal antibodies used for this study, AR4 and RAZ1, bind to separate non-overlapping epitopes of the binding domain of the botulinum toxin,[64] as indicated in Fig. 1. Our simulant, a fragment of the heavy chain that contains the binding domain, includes these epitopes.

The AR4 IgG antibody was covalently bound directly to Sepharose beads of 75–150 μm diameter. In general, we find that this binding approach is preferred over methods using streptavidin/biotin interactions, since the streptavidin becomes a site for significant non-specific binding interactions.[67] The rotating rod flow cell (Fig. 2) for capturing the Sepharose beads has been described previously[43,44] and details for the particular flow cell used for these experiments are provided in the Experimental section. The column packing contains orders of magnitude more moles of capture antibody than the moles of toxin to be captured. For example, a column created from 100 μL of bead suspension prepared and diluted as described in the Experimental section will contain >1000 times more moles of antibody than a 100 μL sample at a 100 pM toxin (or toxin simulant) sample concentration.

The reporter RAZ1 IgG antibody was labeled with Alexa 647 dye. The excitation light from the HeNe laser (633 nm) passed through a laser-line filter and was delivered to the flow cell using an optical fiber. Emission light was collected with a second optical fiber at 90°, filtered through long-wave-pass and band-pass filters primarily to remove scattered excitation light, and detected with a PMT. The overlap of the Alexa 647 dye excitation band with the 633 nm laser line is sufficient for fluorescence, and the Alexa 647 emission band is significantly separated from the laser line wavelength.

Our current instrumentation and reagents represent several improvements over the system we briefly described previously.[14] Fiber optic coupling to the flow cell was redesigned using larger core fibers, better fitting to the flow cell, and a more careful

geometry for excitation and emission. A new optical filter train with high-end filters was set up to improve the rejection of excitation light (described in detail in the Experimental). New amplification circuits were employed for the PMT and the gain was increased. The reagents have also improved. The antibodies were selected from families of affinity-matured monoclonal antibodies. Whereas the capture antibody was previously AR1, with a binding affinity of 22 pM (by Biacore measurements), the current capture antibody was AR4 with a binding affinity of 3 pM. Similarly, we replaced the labeling antibody 3D12 (164 pM) with RAZ1 (3.5 pM). The capture antibodies were covalently linked to NHS-activated beads in the current study rather than using streptavidin coupling, to reduce non-specific binding, as noted above. In addition, we produced fresh BoNT/A-H_C-fragment in-house and assayed it in-house to assure that we were using an antigen that had not denatured.

Renewable surface immunoassay

Once the Sepharose beads with the capture antibodies are trapped in the rotating rod flow cell, the assay consists of a sequence of fluidic operations to deliver the sample, sample wash, reporter antibody, and reporter wash solutions, while logging the fluorescence signal. The basic processes of the assay as well as several salient features are presented in the data traces shown in Fig. 5 and Fig. 6. The sequence of solution deliveries to the flow cell for these experiments is given in Table 2. These figures contain plots for buffer (Fig. 5) and FBS (Fig. 6) sample matrixes.

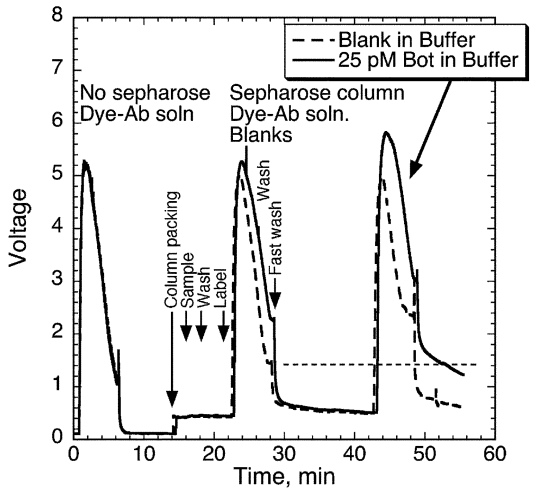

Fig. 5 Fluorescence detection system signals, as voltages, as a function of time for experiments consisting of three consecutive procedures as described in the text. The data traces are shown for blank and toxin fragment standard (25 pM Bot) in buffer. The Alexa 647 dye-labeled antibody solution was at a 1 : 4000 dilution. The capture antibody on the Sepharose beads is AR4 and the reporter antibody is RAZ1. The first procedure has no Sepharose in the flow cell and shows passage of the dye-labled antibody through the flow cell as a peak. At 14 minutes, the second procedure starts with packing the bead column. Both traces at this stage represent blanks, perfusing with the blank sample, wash, labeling antibody, wash and fast wash. The peak shows the passage of the labeling antibody through the packed column, and return to baseline with washing. The packing material is left in the column and the sequence of sample, wash, label, wash, and fast wash is repeated. The dashed trace is a blank and the solid trace is a 25 pM toxin fragment sample for this third procedure.

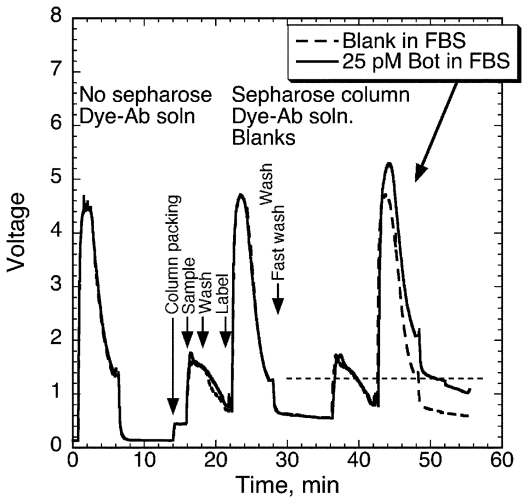

Fig. 6 Detection system signals for three consecutive procedures as shown previously in Fig. 5, but in a matrix fetal bovine serum (FBS). In this matrix the sample perfusion results in a detectable increase in signal voltage prior to the labeling step.

Table 2 Solutions delivered to the renewable surface sensor for the following sequence: perfusion of the flow cell with dye in the absence of a packed column, perfusion in a blank experiment with packed column, and subsequent assay or second blank on the same packed column

Approximate start time (min)	Solution or bead suspension	Volume (μL)	Flow rate[a] (μL/sec)
1	Reporter antibody	100	1
5	Wash 1	25	1
6	Wash 2 (fast wash)	1900	5
14	Beads	120	5
16	Sample (blank)	100	1
20	Wash	75	1
22.5	Reporter antibody	100	1
26.5	Wash 1	25	1
27.5	Wash 2 (fast wash)	1900	5
36.5	Sample (standard or blank)	100	1
42.5	Wash	75	1
43	Reporter antibody	100	1
47	Wash 1	25	1
48	Wash 2 (fast wash)	1900	5
56	Flush beads	500	400

[a] Programmed delays and brief stops in the procedure are not listed. During sample perfusion and reporter antibody perfusion, the fluid was advanced 1 μL at a time at 1 μL/sec, with delays between each such advance to provide increased contact time. Flow was stopped and the 1 mL syringe was refilled prior to the beginning of the fast wash and again at the middle of the fast wash (total 1.9 mL).

Each trace in each plot illustrates three consecutive procedures, resulting in three major fluorescence peaks from the detection of excess reporter antibody solution passing through the flow cell. The first two major peaks are controls or blanks for understanding the assay procedure, and the third peaks include an analysis. The reporter antibody concentration in these demonstration experiments was diluted more than normal (1 : 4000 instead of 1 : 2000) so that the signal would be on scale at all

times. Each plot has two data traces. The solid line trace in each plot contains the analysis of a 25 pM toxin fragment standard as the third and final portion of the trace. The dashed line corresponds to procedures where the third portion is a blank.

For the first peaks at about 2 min there is no Sepharose packing in the flow cell. As the dye-labeled reporter antibody solution zone passes through the sensor a transient signal is observed. The peak is unsymmetrical as is typical in flow or sequential injection analysis system with dispersion of the reagent zone as it passes through tubing, valves, and devices.

The second major peak in Fig. 5 at about 24 min represents a complete assay procedure using blank samples (buffer solution with no toxin fragment) for both traces. The initial packing of the column with antibody-coupled Sepharose raises the baseline signal due to scattered excitation light. Perfusion with a zone of sample blank does not alter the observed signal in experiments in buffer. The sample zone is followed by carrier fluid to wash away the sample matrix. Then the dye-labeled reporter antibody solution zone is perfused through the column, resulting in the major observed fluorescence peak. This solution is followed by a carrier fluid wash. The flow is stopped to reload the syringe, followed by additional washing at a higher flow rate for a fast wash totaling 1.9 mL. The 1 mL syringe is reloaded during a stop in the middle of this wash. The analytical signal is taken as the signal intensity, or the integral of the intensity over time during the fast wash, after the fast wash has removed the bulk of the excess dye-labeled reporter antibody. For these two blanks the peak intensities and widths varied somewhat during reporter antibody perfusion; however, there is little difference in the analytical signal level (as expected for blanks). The columns from these procedures were left in the flow cell for the next and final assays.

Unlike samples delivered in buffer, samples in more complex matrixes can lead to a fluorescence signal during sample perfusion. This is illustrated using the FBS sample matrix in Fig. 6. Sample solutions may lead to signal due to fluorescent components or scattered laser light. However, the column is washed to remove the sample matrix after sample load, which is evident in the declining signal prior to column perfusion with reporter antibody.

The third major peak at about 44 min in Fig. 5 corresponds to the assay procedure in which the solid trace involves a sample containing 25 pM botulinum toxin fragment, while the dashed trace is again a blank sample. (The same procedure was conducted for Fig. 6, but in an FBS sample matrix.) The packed column has not been renewed since the previous blank assay (the second peak in the trace). The sample containing 25 pM botulinum toxin fragment retains dye-labeled reporter antibody, providing an analytical signal that is much greater than that of the blank: the toxin fragment is easily detectable at 25 pM. Throughout months of experiments while we refined our assay procedure and measurement system, we were able to detect 10 pM but could not reliably detect the toxin fragment at the single pM concentration range.

Several features of the analysis are evident in these experiments. The capture of labeled reporter antibody by botulinum toxin fragment (solid trace in the third procedure of Fig. 5 or Fig. 6) is evident in the increased peak height and width during and immediately after the reporter antibody perfusion, as well as the signal level during the fast wash when the bulk of the excess reporter antibody has been removed. Indeed, the peak height during reporter perfusion is greater for the toxin fragment standard by an amount that is similar to the difference between standard and blank after washing, as it should be. In general, however, we have found the analytical signal after removing the bulk of the free reporter during the fast wash to be a more reliable indicator of the amount of specifically captured label than the incremental increase in fluorescence while free label is still in the column, particularly at the lowest toxin fragment concentrations. The analytical signal for the 25 pM sample (solid trace in the third procedure of Fig. 5 or Fig. 6) is higher than either of the blank runs in the dashed line trace or the blank run of the solid trace which preceded the sample run in the solid trace.

The measurement signal consists of the analytical signal of the sample or standard minus the analytical signal of a blank. The plots in Fig. 5 and Fig. 6 suggest more than one approach for assessing the 'analytical signal of the blank'. One could pack a column, run a blank on that column, then run a sample or standard *on the same column*, which would require about 40 minutes. Alternatively, one could run one or more initial blanks to determine the analytical signal of the blank, and then run standards and samples each on its own column. The former approach is more time-consuming per sample, but allows one to subtract a blank *for the same column* as the subsequent sample or standard. If total assay time and throughput are not critical, one could also run a fluorescent standard through the system without a column packed, similar to the first peak in Fig. 5 and Fig. 6. This would provide a quality control check on the effective fluorescence sensitivity of the system just prior to the measurement.

The solid traces in the plots in Fig. 5 and Fig. 6 represent the most time-consuming approach that includes checking fluorescent sensitivity, packing a column, running the blank, and then running standard or sample *on the same packed column*. The horizontal dashed line intersecting the sample analytical signal at about 52 min is provided to facilitate comparison of this sample signal with the prior blank signal at about 32 min (solid trace).

The alternative approach, running standards or samples, each on their own packed column, after having first determined the analytical signal of the blank in separate experiments, provides a more rapid screening approach. The standard and sample runs would each require only 20 min or less, once the blank analytical signal level had been determined. This approach is subject to variation in column packing from run to run; however, the automated sequential injection fluidic procedures and column packing are, in general, reproducible. Rapid screening would trade off precision and reliability near the detection limit in order to obtain higher sample throughput.

Rapid screening procedure

For rapid screening, the assay was calibrated as shown in Table 1, Fig. 7 and Fig. 8. For each standard, a new column was packed and the standard was run. The detector traces shown in Fig. 7 are each the average of three runs, with each trace starting after the column has already been packed with antibody-coupled Sepharose beads. If the peak heights during reporter antibody perfusion were observable, the peaks for each standard

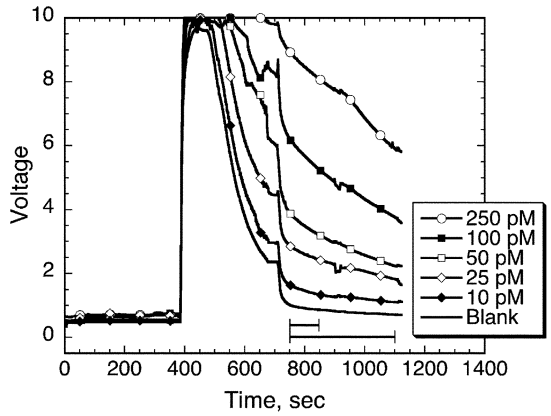

Fig. 7 Assay traces for the analysis of toxin fragment from 0 to 250 pM in the rapid assay approach (see text). Each trace shown is the average of three runs at each concentration, starting the trace after the column has already been packed with antibody-coupled Sepharose beads. The intervals used to integrate the fluorescence signal are shown below the blank trace from 750 to 850 seconds, and from 750 to 1100 seconds.

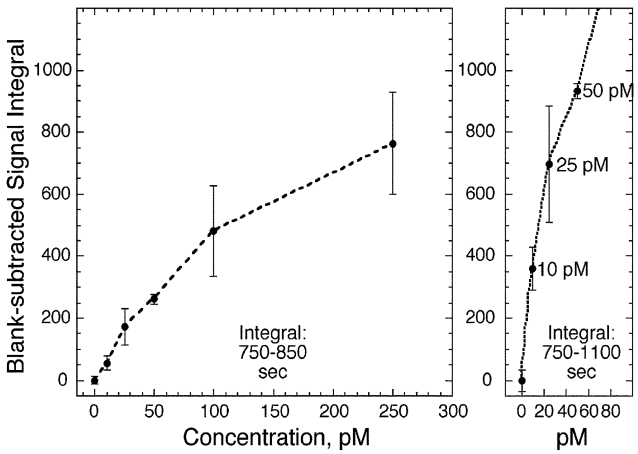

Fig. 8 Calibration curves for the determination of botulinum toxin fragment corresponding to the data in the previous figure. Each data point is the average of three determinations. The value of the blank for subtraction from standard runs was obtained from the average of three initial blank runs. Each blank and standard run was measured with a newly packed column. The signals were integrated from 750 to 850 seconds for the left plot, and from 750 to 1100 seconds for the right plot. The error bars are the standard deviation of the average at each concentration. The data point at 0 pM concentration is the blank level with the standard deviations shown.

concentration would increase in height and width with increasing concentration as the signal from specifically captured dye is added to the signal due to free dye passing through the system. However, the intensity tops out at the 10 V limit of our detection system. The increases in peak *width* with analyte concentration are apparent, as are the increases in signal level after the removal of free dye-labeled antibody during the fast wash.

It is observed that the fluorescence intensity continues to decline for the duration of the fast wash, after the bulk of the free reporter has been removed. This is seen in blank runs as well as standard runs, and is more pronounced in the standard runs at higher toxin concentrations. At 10 pM, the trace essentially parallels the blank trace, but at higher concentrations the slopes become steeper than the blank.

The Sepharose beads are a highly porous hydrogel medium that reagents can diffuse into. They were selected because they have a refractive index that is closer to water than impermeable polymer beads, minimizing light scattering from the column. Sepharose is commonly used in size exclusion or gel permeation chromatography, and is used to separate proteins in the 70–20 000 kDa range. Accordingly, reporter antibody is expected to be removed from the column by a process including washing from the free column volume, as well as much slower diffusion out of the beads into the free column volume, leading to a long asymptotic approach to steady-state as the dye clears the column. In addition, the dye-labeled reporter antibody could be subject to non-specific binding to captured protein, which would retard its diffusion out of the beads; this effect would increase as the toxin concentration increased. Photobleaching of the Alexa 647 dye may also occur.[68] Nevertheless, using control experiments to be described below, we clearly establish that the fluorescent signal during the fast wash after the bulk of the free reporter antibody has been washed away is due to the formation of the sandwich complex and is correlated with the concentration of the toxin.

The values used in the calibration curve are derived by integrating the signal during the fast wash after perfusion with dye-labeled antibody and washing away the bulk of the free dye. The values were determined for an integral from 750 to 850 seconds for the main plot on the left in Fig. 8. The fast wash is continuous with no flow interruptions during this interval; thus this integration period selects an interval after the bulk of the free reporter has been washed out but before the syringe refill in the middle of the fast wash. The signal was integrated from 750 to 1100 seconds for the narrower plot on the right. This longer interval includes a flow interruption as the syringe is refilled, which can lead to blips in the signal that introduce noise in the measurement. This is particularly evident in the 25 and 100 pM traces just after 900 seconds in Fig. 7 (and was observed in the dashed trace in Fig. 5 at 52 minutes), and can introduce random noise into the longer integration period. (However, if longer integration times are desired, changing syringe size or flow operations could be used to avoid such noise, or the flow could simply be stopped for the measurement interval.) At 10 pM concentration, the longer integration period provides increased signal and lower relative standard deviation. The relative standard deviation for the blank-subtracted signal intensity at 10 pM was 42% using the shorter integration time and 19% at the longer integration time. The standard deviation of the blank signals were about half the standard deviation of the signals at 10 pM, regardless of the integration time, and are shown as error bars in Fig. 8. The background-subtracted average signal at 10 pM was 4.4 times the standard deviation of the blank signal at the shorter integration time, and over 10 times at the longer integration time. Comparing instead to the standard deviation of the background-subtracted signal at 10 pM, which is larger than that of the blank, the average signal at 10 pM is 2.4 times the standard deviation using the shorter integration time and 5.2 times the standard deviation using the longer integration time. At 25 pM, where a noticeable blip at the syringe refill introduces noise into the longer integration time, the relative standard deviation was still lower using the longer integration time.

Control experiments

The experiments clearly show that the fluorescent sandwich assay in the renewable surface sensor provided a signal that was dependent on the toxin fragment concentration. Control experiments were run in the sensor flow cell using AR4-coupled Sepharose beads, botulinum toxin fragment at blank, 50, and 100 pM concentrations, and dye-labeled reporter antibodies that are not specific to the toxin fragment. These control experiments were conducted using Alexa 647-labeled donkey anti-sheep IgG or Alexa-633-labeled goat anti-chicken IgG as reporter antibodies. In all control experiments, the background signal was observed as usual and there were no discernible increases in signal with antigen concentration. Thus without both the toxin-specific capture and reporter antibodies, an antigen-dependent signal level was not observed.

In addition, control experiments were run creating the sandwich complex outside the sensor flow cell in 2 mL centrifuge tubes. AR4-coupled Sepharose beads, Alexa 647-labeled RAZ1 antibodies, and toxin fragment were allowed to react for 60 minutes at 4 °C, centrifuged and washed. Then the beads were loaded into the flow cell with the rotating rod in the bead-trap position (shown in Fig. 2), and the signals were determined with the sensor fluorescence detection system while washing the beads at a high flow rate. Using this model system, toxin fragment was detected and the signal was dependent on the toxin fragment concentration. Further, we were able to detect the toxin fragment at concentrations as low as 5 pM. The fluorescence intensity declines with washing as observed in the automated assay. At 5 pM, it took 20 minutes to asymptotically approach horizontal. This is too long to wait for a rapid screening assay; a signal that is proportional to toxin concentration can be determined much earlier in the wash (Fig. 7). It was also noted that at each syringe reload during the extended washing, the signal dropped, and on resuming flow the signal returned to the pre-reload level, leading to 'blips' as noted above. These arise because under high flow, the Sepharose hydrogel beads are compressed, whereas when the flow is stopped, they decompress and the quantity of dye-retaining beads in the optical detection path is reduced. Resuming flow recompresses the beads.

From the control experiments in this section, it can be concluded that the antigen-dependent signal levels in the sensor assay were due to the sandwich assay itself and not some aspect of the flow system and sensor flow cell used to automate the assay and quantify the measurement signal.

Discussion

We have described an automated fluidic sandwich immunoassay designed for moderately fast or very fast screening for traces of botulinum toxin in liquid sample matrixes. This assay features high affinity antibodies and a renewable surface microcolumn sensor flow cell with on-column fluorescence detection. In our prior initial report on this assay approach,[14] the lowest tested concentration of 100 pM was detectable. We now report detection down to 10 pM. We attribute this improvement to the facts that we redesigned the optical geometry and connections to the flow cell, made a much better optical system to reject excitation light and signal over background, we used higher affinity antibodies, and we used a better method of coupling the capture antibody to the beads. Each assay can be completed in less than 20 minutes using the rapid assay procedure, once the blank signal levels have been established by initial blank runs.

Our 10 pM detection limit corresponds to 0.5 ng/mL of toxin fragment (50 kDa) or 1.5 ng/mL of the holotoxin (150 kDa). Given a 100 μL sample volume, this assay detected 50 pg of toxin fragment. Our detection limit compares similarly or favorably to other fluidic biosensor immunoassay approaches that provide detection in 20 minutes or less. The fiber optic evanescent wave immunosensor from the Naval Research Laboratory was reported to have a 30 pM detection limit for botulinum toxin A in an assay that took less than 20 minutes.[31] A fluidic biosensor array has been tested against botulinum *toxoid* A (a deactivated form of the full toxin with lower toxicity) in 20 minute assays yielding detection limits of 20 ng/mL, which would correspond to over 100 pM toxin concentration.[33,34] Recently, using a novel recognition element based on antimicrobial peptides on the biosensor array, a 75 minute assay for the toxoid with a 1 ng/mL detection limit has been reported.[24]

Our assay approach for botulinum toxin is unique in providing new biorecognition surfaces automatically using the renewable surface technique, and our study is further distinguished by using a recombinant fragment of BoNT/A as a structurally valid non-toxic simulant for the holotoxin. In further work, we are examining other methods of labeling the reporter antibody with fluorophores.

Acknowledgements

The authors are grateful for funding from the U.S. Department of Homeland Security. In addition, the antibody development work at UCSF was partially supported by NIAID R21 grant AI53389-01, NIAID cooperative agreement U01 AI056493, and DoD contract DAMD17-03-C-0076. A portion of the research was performed using EMSL, a national scientific user facility sponsored by the Department of Energy's Office of Biological and Environmental Research located at Pacific Northwest National Laboratory. The Pacific Northwest National Laboratory is operated for the U.S. DOE by Battelle Memorial Institute.

References

1 H. Sugiyama, *Microbiol. Rev.*, 1980, **44**, 419–448.
2 L. L. Simpson, *Ann. Rev. Pharmacol. Toxicol.*, 2004, **44**, 167–193.
3 R. Pellizzari, O. Rossetto, G. Schiavo and C. Montecucco, *Philos. Trans. R. Soc. London, Ser. B-Biological Sci.*, 1999, **354**, 259–268.
4 D. B. Lacy, W. Tepp, A. C. Cohen, B. R. DasGupta and R. C. Stevens, *Nat. Struct. Biol.*, 1998, **5**, 898–902.
5 D. B. Lacy and R. C. Stevens, *J. Mol. Biol.*, 1999, **291**, 1091–1104.
6 S. S. Arnon, R. Schechter, T. V. Inglesby, D. A. Henderson, J. G. Bartlett, M. S. Ascher, E. Eitzen, A. D. Fine, J. Hauer, M. Layton, S. Lillibridge, M. T. Osterholm, T. O'Toole, G. Parker, T. M. Perl, P. K. Russell, D. L. Swerdlow and K. Tonat, *JAMA, J. Am. Med. Assoc.*, 2001, **285**, 1059–1070.
7 A. Scarlatos, B. A. Welt, B. Y. Cooper, D. Archer, T. DeMarse and K. V. Chau, *J. Food Sci.*, 2005, **70**, R121–R130.
8 D. A. Kautter and H. M. Solomon, *J. AOAC Int.*, 1977, **60**, 541–545.
9 E. J. Schantz and D. A. Kautter, *J. AOAC Int.*, 1978, **61**, 96–99.
10 S. K. Sharma and R. C. Whiting, *J. Food Prot.*, 2005, **68**, 1256–1263.
11 T. A. N. Ekong, K. McLellan and D. Sesardic, *J. Immunol. Methods*, 1995, **180**, 181–91.
12 M. D. Potter, J. Meng and P. Kimsey, *J. Food Prot.*, 1993, **56**, 856–61.

13 S. K. Sharma, J. L. Ferreira, B. S. Eblen and R. C. Whiting, *Appl. Environ. Microbiol.*, 2006, **72**, 1231–1238.
14 S. M. Varnum, M. G. Warner, B. Dockendorff, N. C. Anheier Jr., J. Lou, J. D. Marks, L. A. Smith, M. J. Feldhaus, J. W. Grate and C. J. Bruckner-Lea, *Anal. Chim. Acta*, 2006, **570**, 137–143.
15 H.-Y. Chao, Y.-C. Wang, S.-S. Tang and H.-W. Liu, *Toxicon*, 2004, **43**, 27–34.
16 M. Wictome, K. Newton, K. Jameson, B. Hallis, P. Dunnigan, E. Mackay, S. Clarke, R. Taylor, J. Gaze, K. Foster and C. Shone, *Appl. Environ. Microbiol.*, 1999, **65**, 3787–3792.
17 M. Wictome, K. A. Newton, K. Jameson, P. Dunnigan, S. Clarke, J. Gaze, A. Tauk, K. A. Foster and C. C. Shone, *FEMS Immunol. Med. Microbiol.*, 1999, **24**, 319–323.
18 J. J. Schmidt, R. G. Stafford and C. B. Millard, *Anal. Biochem.*, 2001, **296**, 130–137.
19 M. Dong, W. H. Tepp, E. A. Johnson and E. R. Chapman, *Proc. Natl. Acad. Sci. USA*, 2004, **101**, 14701–14706.
20 O. Attree, V. Guglielmo-Viret, V. Gros and P. Thullier, *J. Immunol. Methods*, 2007, **325**, 78–87.
21 S.-M. Han, J.-H. Cho, I.-H. Cho, E.-H. Paek, H.-B. Oh, B.-S. Kim, C. Ryu, K. Lee, Y.-K. Kim and S.-H. Paek, *Anal. Chim. Acta*, 2007, **587**, 1–8.
22 S. Ahn-Yoon, T. R. DeCory and R. A. Durst, *Anal. Bioanal. Chem.*, 2004, **378**, 68–75.
23 K. Bagranyan, J. R. Barash, S. s. Arnon and M. Kalkum, *PLoS ONE*, 2008, **3**, e2041.
24 N. V. Kulagina, G. P. Anderson, F. S. Ligler, K. M. Shaffer and C. R. Taitt, *Sensors*, 2007, **7**, 2808–2824.
25 V. R. Rivera, F. J. Gamez, W. K. Keener, J. A. White and M. A. Poli, *Anal. Biochem.*, 2006, **353**, 248–256.
26 V. Guglielmo-Viret, O. Attree, V. Blanco-Gros and P. Thullier, *J. Immunol. Methods*, 2005, **301**.
27 K. Bagramyan, J. R. Barash, S. S. Arnon and M. Kalkum, *PLoS ONE*, 2008, **3**, e2041.
28 J. T. Mason, L. Xu, Z. M. Sheng and T. J. O'Leary, *Nat. Biotechnol.*, 2007, **24**, 555–557.
29 F. Gessler, S. Pagel-Wieder, M. A. Avondet and H. Boehnel, *Diagn. Microbiol. Infect. Dis.*, 2007, **57**, 243–249.
30 S. K. Sharma, B. S. Eblen, R. L. Bull, D. H. Burr and R. C. Whiting, *Applied and Environmental Microbiology*, 2005, **71**, 3935–3941.
31 L. C. Shriver-Lake, R. A. Ogert and F. S. Ligler, *Sens. Actuators*, 1993, **B11**, 239–43.
32 R. A. Ogert, J. E. Brown, B. R. Singh, L. C. Shriver-Lake and F. S. Ligler, *Anal. Biochem.*, 1992, **205**, 306–12.
33 F. S. Ligler, C. R. Taitt, L. C. Shriver-Lake, K. E. Sapsford, Y. Shubin and J. P. Golden, *Anal. Bioanal. Chem.*, 2003, **377**, 469–477.
34 K. E. Sapsford, C. R. Taitt, N. Loo and F. S. Ligler, *Appl. Environ. Microbiol.*, 2005, **71**, 5590–5592.
35 J. Ruzicka and L. Scampavia, *Anal. Chem.*, 1999, **71**, 257A–263A.
36 J. Ruzicka, *Anal. Chim. Acta*, 1995, **308**, 14–19.
37 J. Ruzicka, *Analyst*, 1994, **119**, 1925–1934.
38 C. H. Pollema and J. Ruzicka, *Anal. Chem.*, 1994, **66**, 1825–1831.
39 J. Ruzicka, C. H. Pollema and K. M. Scudder, *Anal. Chem.*, 1993, **65**, 3566–3570.
40 M. D. Luque de Castro, J. Ruiz-Jimenez and J. A. Perez-Serradilla, *Trends Anal. Chem.*, 2008, **27**, 118–126.
41 M. Miro, S. K. Hartwell, J. Jakmunee, K. Grudpan and E. H. Hansen, *Trends Anal. Chem.*, 2008, **27**, 749–761.
42 B. Dockendorff, D. A. Holman, G. D. Christian and J. Ruzicka, *Anal. Commun.*, 1998, **35**, 357–359.
43 C. J. Bruckner-Lea, M. S. Stottlemyre, D. A. Holman, J. W. Grate, F. J. Brockman and D. P. Chandler, *Anal. Chem.*, 2000, **72**, 4135–4141.
44 J. W. Grate, C. J. Bruckner-Lea, A. E. Jarrell and D. P. Chandler, *Anal. Chim. Acta*, 2003, **478**, 85–98.
45 D. P. Chandler, F. J. Brockman, D. A. Holman, J. W. Grate and C. J. Bruckner-Lea, *Trends Anal. Chem.*, 2000, **19**, 314–321.
46 O. Egorov, M. J. O'Hara, J. W. Grate and J. Ruzicka, *Anal. Chem.*, 1999, **71**, 345–352.
47 J. W. Grate and O. B. Egorov, *Anal. Chem.*, 1998, **70**, 779A–788A.
48 C. H. Pollema, J. Ruzicka, G. D. Christian and A. Lernmark, *Anal. Chem.*, 1992, **64**, 1356–61.
49 B. Willumsen, G. Christian and J. Ruzicka, *Anal. Chem.*, 1997, **69**, 3482–3489.
50 A. D. Carroll, L. Scampavia, D. Luo, A. Lernmark and J. Ruzicka, *Analyst*, 2003, **128**, 1157–1162.
51 R. Zhang, K. Hirakawa, M. Katayama, H. Nakajima, N. Soh, K. Nakano and T. Imato, *J. Flow Inject. Anal.*, 2006, **23**, 117–122.
52 H. Kuramitz, M. Dziewatkoski, B. Barnett, H. B. Halsall and W. R. Heineman, *Anal. Chim. Acta*, 2006, **561**, 69–77.
53 R. M. Ozanich, K. C. Antolick, C. J. Bruckner-Lea, B. P. Dockendorff, A. N. Easterday, H. C. Edberg, J. W. Grate, S. Iyer, L. H. Johnson, T. M. Straub, C. O. Valdez and M. G. Warner, *JALA*, 2007, **12**, 303–310.
54 T. M. Straub, B. P. Dockendorff, M. D. Quinonez-Diaz, C. O. Valdez, J. I. Shutthanandan, B. J. Tarasevich, J. W. Grate and C. J. Bruckner-Lea, *J. Microbiol. Methods*, 2005, **62**, 303–316.
55 C. J. Bruckner-Lea, T. Tsukuda, B. Dockendorff, J. C. Follansbee, M. T. Kingsley, C. Ocampo, J. R. Stults and D. P. Chandler, *Anal. Chim. Acta*, 2002, **469**, 129–140.
56 D. P. Chandler, J. Brown, D. R. Call, S. Wunschel, J. W. Grate, D. A. Holman, L. Olson, M. S. Stottlemyre and C. J. Bruckner-Lea, *Int. J. Food Microbiol.*, 2001, **70**, 143–154.
57 D. P. Chandler, B. L. Schuck, F. J. Brockman and C. J. Bruckner-Lea, *Talanta*, 1999, **49**, 969–983.
58 P. Amersdorfer, C. Wong, S. Chen, T. Smith, S. Deshpande, R. Sheridan, R. Finnern and J. D. Marks, *Infect. Immun.*, 1997, **65**, 3743–3752.
59 P. Amersdorfer, C. Wong, T. Smith, S. Chen, S. Deshpande, R. Sheridan and J. D. Marks, *Vaccine*, 2002, **20**, 1640–1648.
60 A. Nowakowski, C. Wang, D. B. Powers, P. Amersdorfer, T. J. Smith, V. A. Montgomery, R. Sheridan, R. Blake, L. A. Smith and J. D. Marks, *Proc. Natl. Acad. Sci. USA*, 2002, **99**, 11346–11350.
61 A. Razai, C. Garcia-Rodriguez, J. Lou, I. N. Geren, C. M. Forsyth, Y. Robles, R. Tsai, T. J. Smith, L. A. Smith, R. W. Siegel, M. Feldhaus and J. D. Marks, *J. Mol. Biol.*, 2005, **351**, 158–169.
62 T. J. Smith, J. Lou, I. N. Geren, C. M. Forsyth, R. Tsai, S. L. LaPorte, W. H. Tepp, M. Bradshaw, E. A. Johnson, L. A. Smith and J. D. Marks, *Infect. Immun.*, 2005, **73**, 5450–5457.
63 C. Garcia-Rodriguez, R. Levy, J. W. Arndt, C. M. Forsyth, A. Razai, J. Lou, I. N. Geren, R. C. Stevens and J. D. Marks, *Nat. Biotechnol.*, 2007, **25**, 107–116.
64 R. Levy, C. M. Forsyth, S. L. LaPorte, I. N. Geren, L. A. Smith and J. D. Marks, *J. Mol. Biol.*, 2007, **365**, 196–210.
65 M. P. Byrne, T. J. Smith, V. A. Montgomery and L. A. Smith, *Infect. Immun.*, 1998, **66**, 4817–4822.
66 M. A. Clayton, J. M. Clayton, D. R. Brown and J. L. Middlebrook, *Infect. Immun.*, 1995, **63**, 2738–2742.
67 R. Alon, E. A. Bayer and M. Wilchek, *Biochem. Biophys. Res Commun.*, 1990, **170**, 1236–1241.
68 R. M. Thomas, C. A. Nechamen, J. E. Mazurkiewicz, M. Muda, S. Palmer and J. A. Diaz, *Endocrinology*, 2007, **148**, 1987–1995.

